Presented at the COMSOL Conference 2009 Milan

Calculus of the Elastic Properties of a Beam Cross-Section

Alessandra Genoese, Andrea Genoese, Giovanni Garcea

Dipartimento di Modellistica per l'Ingegneria
Università degli Studi della Calabria (Italy)

COMSOL Conference Milan 2009

Subjects

Introduction

The classical linear elastic solutions, as the Saint-Venànt one for slender bodies, can be exploited to generate frame–invariant nonlinear modelings due to the recent proposal of the Implicit Corotational Method.

Subjects

Introduction

The classical linear elastic solutions, as the Saint-Venànt one for slender bodies, can be exploited to generate frame–invariant nonlinear modelings due to the recent proposal of the Implicit Corotational Method.

Implicit Corotational Method (ICR)

ICR splits the motion of the neighbor of each continuum point (or of the cross-section in the case of beam structures) in

- a rigid part filtered through a change of observer
- a strain part considered small and described using linear solutions

Subjects

Introduction

The classical linear elastic solutions, as the Saint-Venànt one for slender bodies, can be exploited to generate frame–invariant nonlinear modelings due to the recent proposal of the Implicit Corotational Method.

Implicit Corotational Method (ICR)

ICR splits the motion of the neighbor of each continuum point (or of the cross-section in the case of beam structures) in

- a rigid part filtered through a change of observer
- a strain part considered small and described using linear solutions

The aims of this work are

- the calculus of the elastic properties of a beam cross-section through the numerical solution of Saint-Venànt problem as proposed in [2];
- the use of the coefficients so evaluated in geometric nonlinear analysis of 3D beam structures as proposed in [1].

The stress distribution

Saint-Venànt cylinder

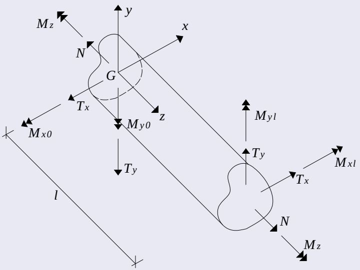

The stress distribution

Saint-Venànt cylinder

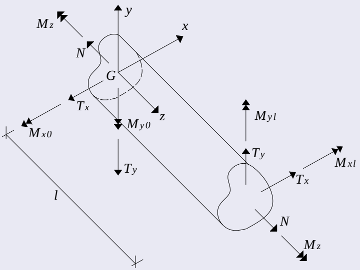

- the cylindrical isotropic body is subjected to surface loading on its end sections
- the local barycentric Cartesian system is oriented according to the principal directions of the cross-section

Saint-Venànt assumptions imply

$$\sigma_{xx} = \sigma_{yy} = \tau_{xy} = 0$$

.

The stress distribution

Saint-Venànt cylinder

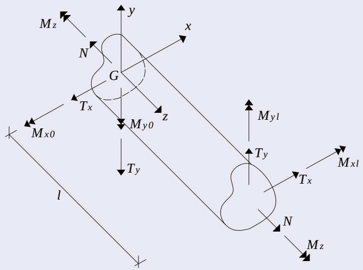

- the cylindrical isotropic body is subjected to surface loading on its end sections
- the local barycentric Cartesian system is oriented according to the principal directions of the cross-section

Saint-Venànt assumptions imply

$$\sigma_{xx} = \sigma_{yy} = \tau_{xy} = 0$$

.

The not zero stress components

$$\sigma_{zz} = \mathbf{D}_\sigma \mathbf{t}_\sigma \ , \quad \boldsymbol{\tau} = \left\{ \begin{array}{c} \tau_{xz} \\ \tau_{yz} \end{array} \right\} = \mathbf{D}_\tau \mathbf{t}_\tau$$

The stress distribution

where

$$\mathbf{t}_\sigma = \begin{Bmatrix} N \\ M_x[z] \\ M_y[z] \end{Bmatrix} \quad \mathbf{t}_\tau = \begin{Bmatrix} T_x \\ T_y \\ M_z \end{Bmatrix}$$

$$\mathbf{D}_\sigma = \begin{bmatrix} 1/A, & y/J_x, & -x/J_y \end{bmatrix}$$

$$\mathbf{D}_\tau = \begin{bmatrix} \mathbf{d}_x, & \mathbf{d}_y, & \mathbf{d}_z \end{bmatrix}$$

$$\begin{cases} \mathbf{d}_x = \nabla\psi_x - \mathbf{b}_x - r_x \mathbf{d}_z \\ \mathbf{d}_y = \nabla\psi_y - \mathbf{b}_y - r_y \mathbf{d}_z \\ \mathbf{d}_z = (\nabla\psi_z - \mathbf{b}_z)/r_z \end{cases}$$

$$\mathbf{b}_x = \frac{1}{2\,J_y} \begin{Bmatrix} x^2 - \bar{\nu} y^2 \\ 0 \end{Bmatrix}$$

$$\mathbf{b}_y = \frac{1}{2\,J_x} \begin{Bmatrix} 0 \\ y^2 - \bar{\nu} x^2 \end{Bmatrix}$$

$$\mathbf{b}_z = \frac{1}{2} \begin{Bmatrix} y \\ -x \end{Bmatrix}$$

$$r_j = 2 \int_A \{\mathbf{b}_j - \nabla\psi_j\}^T \mathbf{b}_z dA,$$

$$j = x, y, z.$$

The stress distribution

where

$$\mathbf{t}_\sigma = \begin{Bmatrix} N \\ M_x[z] \\ M_y[z] \end{Bmatrix} \quad \mathbf{t}_\tau = \begin{Bmatrix} T_x \\ T_y \\ M_z \end{Bmatrix}$$

$$\mathbf{D}_\sigma = \begin{bmatrix} 1/A, & y/J_x, & -x/J_y \end{bmatrix}$$

$$\mathbf{D}_\tau = \begin{bmatrix} \mathbf{d}_x, & \mathbf{d}_y, & \mathbf{d}_z \end{bmatrix}$$

$$\begin{cases} \mathbf{d}_x = \nabla\psi_x - \mathbf{b}_x - r_x\mathbf{d}_z \\ \mathbf{d}_y = \nabla\psi_y - \mathbf{b}_y - r_y\mathbf{d}_z \\ \mathbf{d}_z = (\nabla\psi_z - \mathbf{b}_z)/r_z \end{cases}$$

N, T_x, T_y: normal and shear forces, $M_x[z]$, $M_y[z]$, M_z: bending couples and torque,
A, J_x and J_y: cross- section area and inertia moments,
∇: gradient operator in the $\{x, y\}$ plane.

$$\mathbf{b}_x = \frac{1}{2\,J_y}\begin{Bmatrix} x^2 - \bar{\nu}y^2 \\ 0 \end{Bmatrix}$$

$$\mathbf{b}_y = \frac{1}{2\,J_x}\begin{Bmatrix} 0 \\ y^2 - \bar{\nu}x^2 \end{Bmatrix}$$

$$\mathbf{b}_z = \frac{1}{2}\begin{Bmatrix} y \\ -x \end{Bmatrix}$$

$$r_j = 2\int_A \{\mathbf{b}_j - \nabla\psi_j\}^T \mathbf{b}_z dA,$$

$$j = x, y, z.$$

$\bar{\nu} = \nu/(1+\nu)$ depends on the Poisson coefficient ν of the material.

The stress distribution

The Neumann-Dini problems

Functions ψ_j have to satisfy the Laplace equation for three different Neumann boundary conditions:

$$\begin{cases} \dfrac{\partial^2 \psi_j}{\partial x^2} + \dfrac{\partial^2 \psi_j}{\partial y^2} = 0, \text{ on } A \\ \dfrac{\partial \psi_j}{\partial x} n_x + \dfrac{\partial \psi_j}{\partial y} n_y = \mathbf{b}_j^T \mathbf{n}, \text{ on } \Gamma \end{cases}$$

$\mathbf{n} = \{n_x, \, n_y\}^T$ is the external normal to the cross-section contour Γ.

The stress distribution

The Neumann-Dini problems

Functions ψ_j have to satisfy the Laplace equation for three different Neumann boundary conditions:

$$\begin{cases} \dfrac{\partial^2 \psi_j}{\partial x^2} + \dfrac{\partial^2 \psi_j}{\partial y^2} = 0, \text{ on } A \\ \dfrac{\partial \psi_j}{\partial x} n_x + \dfrac{\partial \psi_j}{\partial y} n_y = \mathbf{b}_j^T \mathbf{n}, \text{ on } \Gamma \end{cases}$$

$\mathbf{n} = \{n_x,\ n_y\}^T$ is the external normal to the cross-section contour Γ.

Remark

- the axial and bending factors can be easily obtained
- the description of the torsional and shear behavior requires the solution of a system of partial differential equations

Cross-section flexibility matrixes

The complementary strain unitary energy

The elastic properties of the cross-section are defined through the energy balance

$$\frac{\partial \phi}{\partial z} = \frac{1}{2E}\int_A \sigma_{zz}^2 \, dA + \frac{1}{2G}\int_A \boldsymbol{\tau}^T \boldsymbol{\tau} \, dA = \frac{1}{2E}\mathbf{t}_\sigma^T \mathbf{H}_\sigma \mathbf{t}_\sigma \; + \frac{1}{2G}\mathbf{t}_\tau^T \mathbf{H}_\tau \mathbf{t}_\tau ,$$

where E and $G = \dfrac{E}{2(1+\nu)}$ are the Young and the tangential elasticity coefficients of the material,

$$\mathbf{H}_\sigma = \int_A \mathbf{D}_\sigma^T \mathbf{D}_\sigma \, dA \, , \quad \mathbf{H}_\tau = \int_A \mathbf{D}_\tau^T \mathbf{D}_\tau \, dA$$

or, for components

$$\mathbf{H}_\sigma = diag\left[\frac{1}{A}\, , \quad \frac{1}{J_x}\, , \quad \frac{1}{J_y}\right] \, , \quad H_{\tau ij} = \int_A \mathbf{d}_i^T \mathbf{d}_j \, dA.$$

The shear and torsional factors A_x^*, A_y^*, J_t used in technical applications

The shear system

In the case of symmetric cross-sections, $\mathbf{H}_\tau$ is a diagonal matrix:

$$\mathbf{H}_\tau = diag\left[\frac{1}{A_x^*}\,,\quad \frac{1}{A_y^*}\,,\quad \frac{1}{J_t}\right].$$

In the hypothesis of general cross-section the shear unitary energy is composed of three independent contributions only in the shear principal system defined by

$$x_c = -\frac{H_{\tau 23}}{H_{\tau 33}}\,,\quad y_c = \frac{H_{\tau 13}}{H_{\tau 33}},$$

$$\tan\alpha_t = \frac{c_2 - c_1 + \sqrt{c_2^2 - 2c_1c_2 + c_1^2 + 4c_3^2}}{2c_3},$$

$$c_1 = H_{\tau 11} - 2H_{\tau 13}\,y_c + H_{\tau 33}\,y_c^2\,,\quad c_2 = H_{\tau 22} + 2H_{\tau 23}\,x_c + H_{\tau 33}\,x_c^2,$$

$$c_3 = H_{\tau 12} + H_{\tau 13}\,x_c - H_{\tau 23}\,y_c - H_{\tau 33}\,x_c y_c.$$

The shear and torsional factors A_x^*, A_y^*, J_t used in technical applications

The shear system

Let's denote with

$$\bar{T}_x = T_x\, c + T_y\, s\ , \quad \bar{T}_y = -T_x\, s + T_y\, c\ , \quad \bar{M}_z = M_z + T_x\, y_c - T_y\, x_c$$

the shear strengths and the torque in shear system,
c and s being the cosine and the sine of the angle α_t.
The energy is then

$$\frac{\partial \phi_T}{\partial z} = \frac{1}{2G}\left\{ \frac{\bar{T}_x^2}{A_x^*} + \frac{\bar{T}_y^2}{A_y^*} + \frac{\bar{M}_z^2}{J_t} \right\},$$

where

$$A_x^* = \frac{1}{c_1\, c^2 + c_2\, s^2 + 2\, c_3\, c\, s}\ , \quad A_y^* = \frac{1}{c_1\, s^2 + c_2\, c^2 - 2\, c_3\, c\, s}\ , \quad J_t = \frac{1}{H_{33}}$$

are the necessary shear and torsional factors.

Calculus of the shear flexibility matrix through COMSOL Multiphysics

The modulus COMSOL Multiphysics-PDE

The following quantities are defined:

- A 2D geometry in which x and y are the independent variables;
- ν and $\bar{\nu}$ as constants;
- The three terms $\mathbf{b}_j^T\mathbf{n}$ as Boundary Expressions;
- Quantities useful to obtain the area, the inertia moments and the expressions of r_j between the Integration Coupling Variables on the domain;
- The components of vectors $\mathbf{d}_j$ and the dot products $\mathbf{d}_i^T\mathbf{d}_j$ on the domain;
- The three differential Laplace equations for the domain and the Neumann conditions for the contour;
- A mesh for the domain using Lagrange-Quadratic elements.

Having found the ψ_j functions, the Postprocessing menu is very useful to evaluate the integrals $H_{\tau ij}$.

Validation tests

Rectangular and Trapezoidal cross-sections

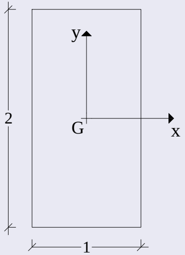

	$\nu = 0$	$\nu = 0.3$	$\nu = 0.5$
k_x	1.2000	1.2748	1.3561
k_y	1.2000	1.2006	1.2012
k_t		1.8220	

The numerical values of $k_x = \dfrac{A}{A_x^*}$, $k_y = \dfrac{A}{A_y^*}$, $k_t = \dfrac{J_p}{J_t}$

are in perfect agreement with the available analytical values:
$k_x = k_y = 6/5$ for $\nu = 0$ $k_t = 1.8220$ for any ν.
$J_p = \int_A (x^2 + y^2) dA$ is the polar inertia.

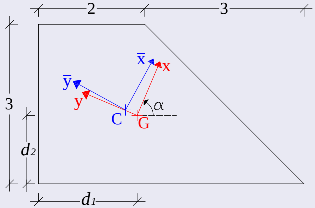

	$\nu = 0$	$\nu = 0.3$	$\nu = 0.5$
k_x	1.3468	1.3771	1.4100
k_y	1.1841	1.1856	1.1871
k_t		1.6481	
x_c		0.0091	
y_c		0.2429	
α_t (*rad*)	-0.0996	-0.0847	-0.0729

The flexural system indicated in red is defined by $d_1 = 1.8571$, $d_2 = 1.2857$, $\alpha = 1.1695\, rad$. It does not coincide with the shear system indicated in blue. Numerical results agree with those proposed in [2].

Validation tests

C-shaped thin walled section and Bridge section

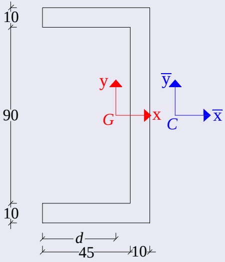

	$\nu = 0$	$\nu = 0.3$	$\nu = 0.5$
k_x	2.8614	2.8716	2.8826
k_y	2.2693	2.2693	2.2693
k_t		59.0380	
x_c		30.3727	

The barycentric system is defined by $d = 37.6250$.

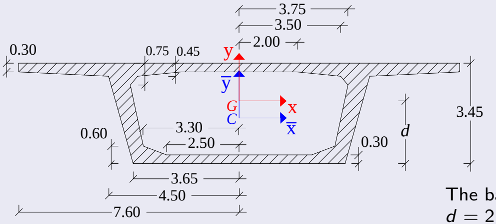

	$\nu = 0.3$
k_x	1.6686
k_y	4.3291
k_t	4.4489
y_c	-0.5863

The barycentric system is defined by $d = 2.1552$.

Comparison tests

C-shaped beam under axial force

COMSOL was used in performing the calculus of the compliance operators $\mathbf{H}_\sigma$ and $\mathbf{H}_\tau$ for the C-shaped section. The analysis was performed using the codes proposed in [1] and through ABAQUS where the cantilever was modeled as a plate-assemblage.

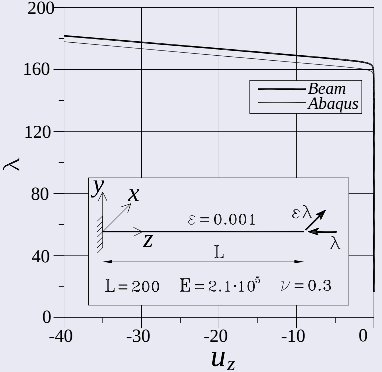

Geometry and equilibrium path. Axial displacement u_z at the edge of the beam

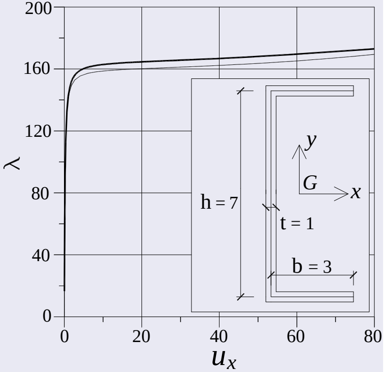

Geometry and equilibrium path. Lateral displacement u_x at the edge of the beam

Comparison tests

C-shaped beam under shear force

In this case too the equilibrium paths obtained through the beam model agree with those furnished by ABAQUS.

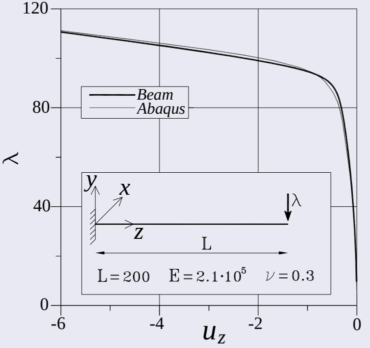

Geometry and equilibrium path. Axial displacement u_z at the edge of the beam

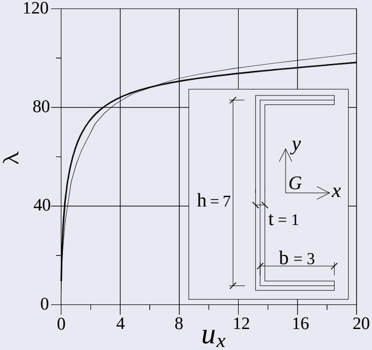

Geometry and equilibrium path. Lateral displacement u_x at the edge of the beam

Conclusion

Conclusion

- ICR allows to generate a nonlinear 3D beam model that contains information gained from Saint-Venànt solution;
- The possibility to evaluate the beam section elastic compliance matrixes in a simple way and reuse these quantities gives a series of advantages in nonlinear analysis of 3D beam structures with respect to the classical beam models;
- In [1] a mixed 3D beam element is proposed. The numerical results agree with those furnished by more complex structural modelings such as the shell one.

Conclusion

Conclusion

- ICR allows to generate a nonlinear 3D beam model that contains information gained from Saint-Venànt solution;
- The possibility to evaluate the beam section elastic compliance matrixes in a simple way and reuse these quantities gives a series of advantages in nonlinear analysis of 3D beam structures with respect to the classical beam models;
- In [1] a mixed 3D beam element is proposed. The numerical results agree with those furnished by more complex structural modelings such as the shell one.

References

G. Garcea, A. Madeo, R. Casciaro
The implicit corotational method, Part *I*/*II*, submitted to Computer Methods in Applied Mechanics and Engineering

A. S. Petrolo R. Casciaro
3d beam element based on Saint-Venànt rod theory, Computers & Structures, 82, pp. 2471-2481, (2004)